



GRID CONNECTED HYBRID POWER SYSTEM FOR DISTRIBUTED GENERATION

Muqthiar Ali Shaik Asst.Professor, Department of Electrical and Electronics Engineering, AITS
RAJAMPET

Abstract

Today, energy is crucial in industrial, residential, agricultural, and electrical sectors. Power generation is a measure of economic progress. Both renewable and non-renewable energy sources may create power. Fossil fuels, oils, etc. are non-renewable resources that pollute and deplete in a few years. Using eco-friendly renewable energy sources to generate electricity may overcome these difficulties. Solar, wind, tidal, waves, etc. are renewable energy sources. Unfortunately, these sources are sporadic and unreliable. Integrated power sources solve this issue. Presented a hybrid integrated architecture for distributed generation using wind and solar energy. It feeds a minimal quantity of electricity into the grid under all situations as an uninterruptible power source. Proposed hybrid wind/photovoltaic energy system converter topology. This topology combines Cuk and SEPIC converters. This setup lets the two energy sources serve the load either separately or concurrently, depending on their availability. Due to its design, this Cuk-SEPIC fused converter does not need high-frequency harmonic filters. Power Factor converters Sepic and Cuk With maximum power point tracking (MPPT) methods, discontinuous conduction mode preregulators (PFP) may boost power transfer efficiency. MATLAB/Simulink developed and tested the suggested model. Verifying the findings concludes.

1.Introduction

Many are seeking sustainable energy alternatives to protect the environment from global warming and fossil fuel depletion. Other than hydropower, wind and photovoltaic energy may suit our energy needs well. Wind energy alone can provide a lot of power, but it's unpredictable.

Solar energy is available all day, although irradiation levels fluctuate owing to light intensity and unexpected shadows from clouds, birds, trees, etc. Wind and photovoltaic systems are sporadic and unstable. However, integrating these two intermittent sources and using MPPT algorithms may boost power transfer efficiency and dependability.



2. Literature Work

Research on grid-connected hybrid power systems for distributed generation spans various aspects, from system design and integration to control strategies and performance evaluation. Here's a breakdown of some notable literature works in this field:

Islam et al provides a comprehensive review of optimal sizing methodologies for hybrid renewable energy systems (HRES) in microgrids, considering factors such as reliability, cost, and environmental impact. It discusses various optimization techniques and tools used for sizing hybrid systems and highlights challenges and future research directions.

Mahmud et al. (2018): focuses on energy management systems (EMS) for microgrids, including grid-connected hybrid systems. It discusses different EMS architectures, control strategies, and optimization methods for coordinating renewable energy sources, energy storage, and loads in microgrid operation. The paper also addresses challenges related to grid interaction and integration with the main grid.

Kumar et al. (2019): This review paper surveys various control strategies employed in distributed generation systems, including grid-connected hybrid power systems. It covers traditional and advanced control techniques for power flow control, voltage regulation, frequency control, and islanding detection in distributed generation systems. The paper discusses the advantages and limitations of different control strategies and identifies areas for further research.

Pourmousavi Kani et al. (2020) presents a review of optimal sizing and operation methodologies for grid-connected hybrid renewable energy systems, considering uncertainties associated with renewable energy resources and load demand. It discusses stochastic optimization techniques, probabilistic modeling approaches, and scenario-based methods for addressing uncertainties in system design and operation. The review also covers challenges related to uncertainty quantification and robust decision-making in hybrid system planning.

Sharma et al. (2021) presents a case study-based performance evaluation of grid-connected hybrid power systems in different geographic locations and application contexts. It analyzes the technical, economic, and environmental performance of hybrid systems using empirical data collected from field trials and operational experiences. The case studies



highlight the benefits, challenges, and lessons learned from real-world deployments of grid-connected hybrid systems.

Nguyen et al. (2022): review explores the impact of energy storage systems (ESS) on the integration of renewable energy sources (RES) in grid-connected microgrids, focusing on system stability, reliability, and economic viability. It discusses the role of ESS in mitigating RES intermittency, enhancing grid stability, and optimizing microgrid operation. The paper also evaluates the techno-economic performance of ESS-integrated microgrids through case studies and simulation studies.

These literature works offer valuable insights into various aspects of grid-connected hybrid power systems for distributed generation, including system design, control strategies, optimization methods, performance evaluation, and real-world applications. Researchers and practitioners in the field can benefit from the findings and recommendations presented in these works to advance the development and deployment of grid-connected hybrid power systems.

3. PROPOSED MULTI-INPUT RECTIFIER STAGE

A system diagram of the proposed rectifier stage of a hybrid energy system is shown in Figure 3.1, where output of the PV array is given as input to the CUK converter and the output of wind generator after converting into dc is given as input to the SEPIC converter. The fusion of the two converters is achieved by reconfiguring the two existing diodes from each converter and the shared utilization of the Cuk output inductor by the SEPIC converter.

This configuration allows the system to operate in both individual and simultaneous mode. It also allows each converter to operate individually in the event that one source is unavailable.

In this case, $M1$ turns off and $M2$ turns on; the proposed circuit becomes a SEPIC converter and the input to output voltage relationship is given by (1). On the other hand, if only the PV source is available, then $M2$ turns off and $M1$ will always be on and the circuit becomes a Cuk converter as shown in Figure . The input to output voltage relationship is given by (2). In both cases, both converters have step-up/down capability, which provide more design flexibility in the system if duty ratio control is utilized to perform MPPT control.

$$V_{dc} / V_w = d_2 / (1-d_2) \quad \text{Eqn.(1)}$$

$$V_{dc} / V_{pv} = d_1 / (1-d_1) \quad \text{Eqn.(2)}$$

Figure 1 illustrates the various switching states of the proposed converter. If the turn on duration of $M1$ is longer than $M2$, then the switching states will be state I, III, IV. Similarly, the switching states will be state I, II, IV if the switch conduction periods are vice versa.

To provide a better explanation, the inductor current waveforms of each switching state are given as follows assuming that $d2 > d1$; hence only states I, III, IV are discussed in this example. In the following, $I_{i,PV}$ is the average input current from the PV source; $I_{i,W}$ is the RMS input current after the rectifier (Wind case); and I_{dc} is the average system output current. The key waveforms that illustrate the switching states in this example are shown in Figure 5.6. The mathematical expression that relates the total output voltage and the two input sources will be illustrated in the next section.

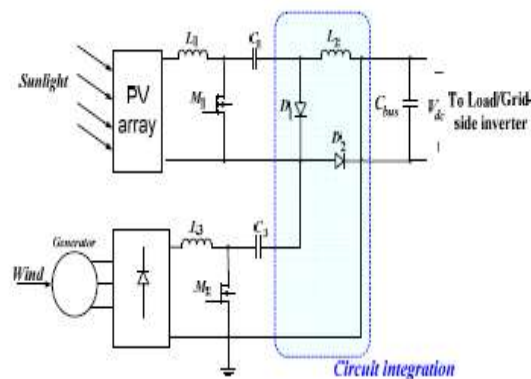


Figure.1:Proposed Multi-InputRectifier

State I (M1 ON, M2 ON):

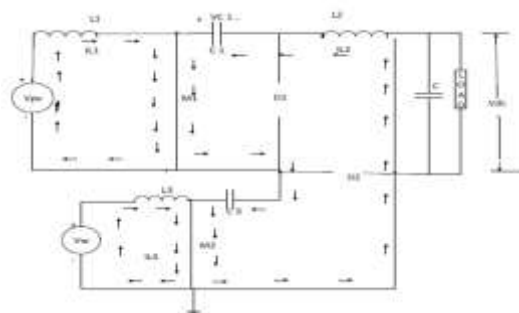


Figure 2.Both PV and Wind sources are present

Currents for State 1:

$$i_{L1} = I_{i,pv} + (v_{pv}/L1)t \quad \text{Eqn.(3)}$$

$$i_{L2} = I_{dc} + (V_{c1} + V_{c2}/L_2)t \quad \text{Eqn.(4)}$$

$$i_{L3} = i_{i,w} + (V_w/L_3)t \quad \text{Eqn.(5)}$$

State II (M1 ON, M2 OFF):

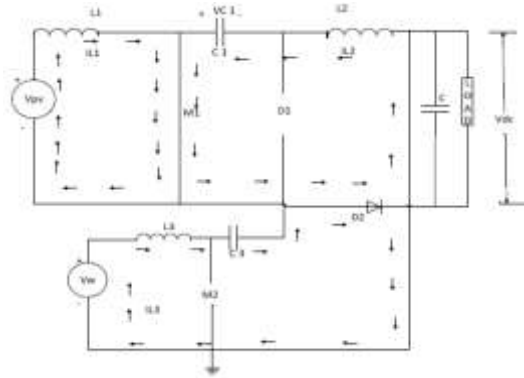


Figure 3 : Only PV Source Operation(CUK)

Currents for State 2:

$$i_{L1} = I_{i,pv} + (V_{pv}/L_1)t \quad \text{Eqn.(6)}$$

$$i_{L2} = I_{dc} + (V_{c1}/L_2)t \quad \text{Eqn.(7)}$$

$$i_{L3} = I_{i,w} + (V_w - V_{c3}/L_3)t \quad \text{Eqn.(8)}$$

State III (M1 OFF, M2 ON):

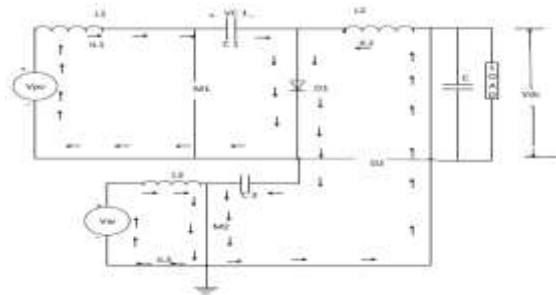


Figure 4 : Only Wind Source Operation(SEPIC)

Currents for State 3:

$$i_{L1} = I_{i,pv} + (V_{pv} - V_{c1}/L_1)t \quad \text{Eqn.(9)}$$

$$i_{L2} = I_{dc} + (V_{c2}/L_2)t \quad \text{Eqn.(10)}$$

$$i_{L3} = I_{i,w} + (V_w/L_3)t \quad \text{Eqn.(11)}$$

State IV (M1 OFF, M2 OFF):

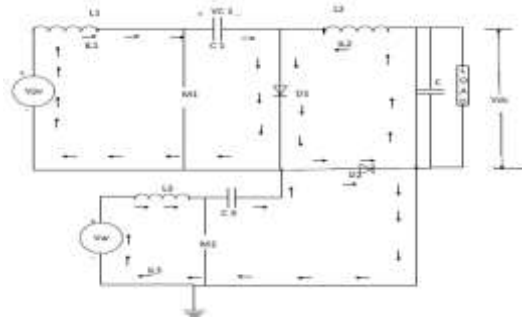


Figure 5.5: Both sources are unavailable

Currents for State 4:

$$i_{L1} = I_{i,pv} + (V_{pv} - V_{c1} / L_1)t \quad \text{Eqn.(12)}$$

$$i_{L2} = I_{dc} - (V_{dc} / L_2)t \quad \text{Eqn.(13)}$$

$$i_{L3} = I_{i,w} + (V_w - V_{c2} - V_{dc} / L_3)t \quad \text{Eqn.(14)}$$

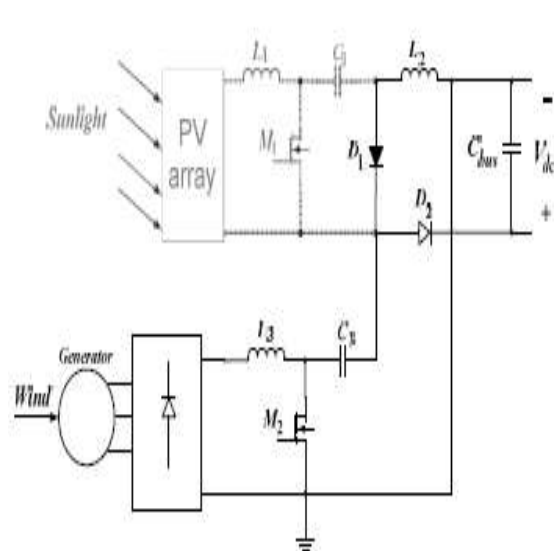
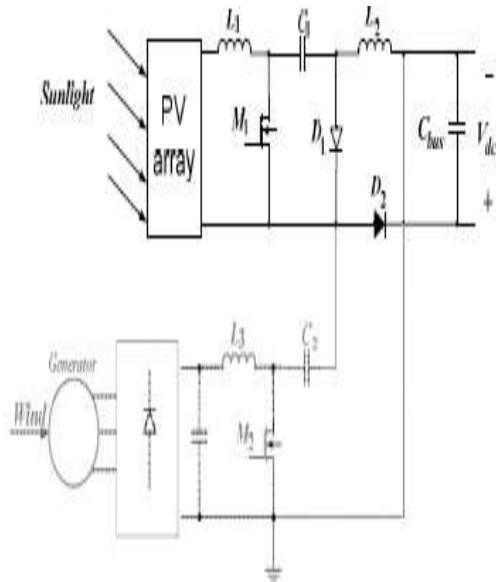


Figure 6 : Only Pv Array Operation(Cuk)

Figure 7 : Only Wind Source Operation(SEPIC)

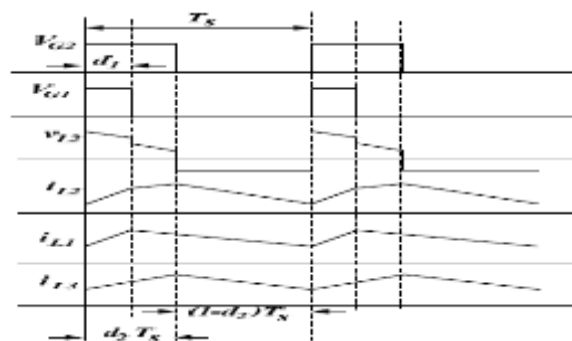


Figure 5.8: Proposed circuit inductor waveforms

4.MPPT CONTROL OF PROPOSED CIRCUIT

A common inherent drawback of Wind and PV systems is the intermittent nature of their energy sources. Wind energy is capable of supplying large amounts of Power but its presence is highly unpredictable as it can be here one moment and gone in another. Solar energy is present throughout the day, but the Solar irradiation levels vary due to sun intensity and unpredictable shadows cast by clouds, birds, trees, etc. These drawbacks tend to make these renewable systems inefficient. However, by incorporating maximum Power point tracking (MPPT) algorithms, the systems' Power transfer efficiency can be improved significantly. To describe a Wind turbine's Power characteristic, equation (15) describes the mechanical Power that is generated by the Wind.

$$P_m = 0.5\rho AC_p (\lambda, \beta) v_w^3 \quad \text{Eqn.(15)}$$

The Power coefficient (C_p) is a nonlinear function that represents the efficiency of the Wind turbine to convert Wind energy into mechanical energy. It is dependent on two variables, the tip speed ratio (TSR) and the pitch angle. The TSR, λ , refers to a ratio of the turbine angular speed over the Wind speed. The mathematical representation of the TSR is given by (16).

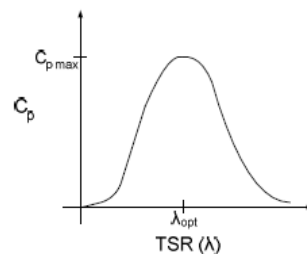


Figure 9: Power Coefficient Curve for a typical Wind turbine

The pitch angle, β , refers to the angle in which the turbine blades are aligned with respect to its longitudinal axis.

Where $\lambda = R \omega_b / V_w$ Eqn.(16)

R = turbine radius,

ω_b = angular rotational speed

Figure 9 and 10 are illustrations of a Power coefficient curve and Power curve for a typical fixed pitch ($\beta=0$) horizontal axis Wind turbine. It can be seen from figure 9 and 10 that the Power curves for each Wind speed has a shape similar to that of the Power coefficient curve. Because the TSR is a ratio between the turbine rotational speed and the Wind speed, it follows

that each Wind speed would have a different corresponding optimal rotational speed that gives the optimal TSR.

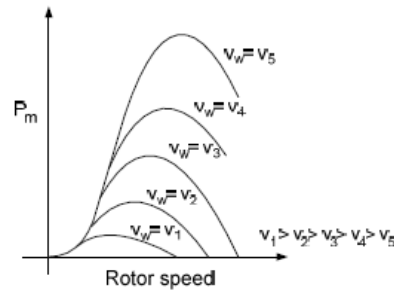


Figure 10: Power Curves for a typical Wind turbine

For each turbine there is an optimal TSR value that corresponds to a maximum value of the Power coefficient ($C_{p,max}$) and therefore the maximum Power. Therefore by controlling rotational speed, (by means of adjusting the electrical loading of the turbine generator) maximum Power can be obtained for different Wind speeds. A Solar cell is comprised of a P-N junction semiconductor that produces currents via the Photovoltaic effect.

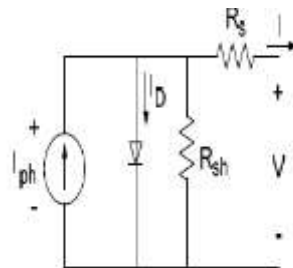


Figure 11: PV cell equivalent circuit

PV arrays are constructed by placing numerous Solar cells connected in series and in parallel. A PV cell is a diode of a large-area forward bias with a Photo voltage and the equivalent circuit is shown by Figure 10. The current-voltage characteristic of a Solar cell is derived in as follows:

$$I = I_{ph} - I_D \tag{Eqn.(17)}$$

$$I = I_{ph} - I_0 [\exp (q(V+R_s I) / AK_B T) - 1] - ((V + R_s I) / R_{sh}) \tag{Eqn.(18)}$$

Where

I_{ph} = Photocurrent,

I_D = diode current,

I_0 = saturation current,

A = ideality factor,

q = electronic charge 1.6×10^{-19} ,

kB = Boltzmann's gas constant (1.38×10^{-23}),

T = cell temperature,

R_s = series resistance,

R_{sh} = shunt resistance,

I = cell current,

V = cell voltage

Typically, the shunt resistance (R_{sh}) is very large and the series resistance (R_s) is very small. Therefore, it is common to neglect these resistances in order to simplify the Solar cell model. The resultant ideal voltage-current characteristic of a Photovoltaic cell is given by (19) and illustrated by Figure 10.

$$I = I_{ph} - I_0(\exp(qv/kt) - 1) \quad \text{Eqn.(19)}$$

The typical output Power characteristics of a PV array under various degrees of irradiation is illustrated by Figure 5.11. It can be observed in Figure 11 that there is a particular optimal voltage for each irradiation level that corresponds to maximum output Power.

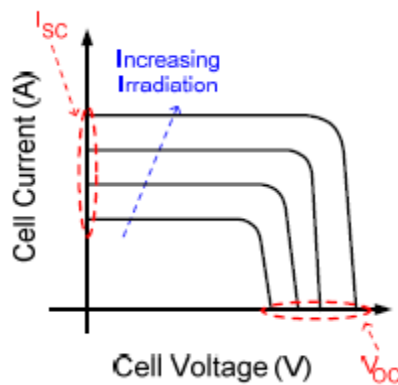


Figure 11 : PV V-I Characteristics

Therefore, by adjusting the output current (or voltage) of the PV array, maximum Power from the array can be drawn. Due to the similarities of the shape of the Wind and PV array Power curves, a similar maximum Power point tracking scheme known as the hill climb search (HCS) strategy is often applied to these energy sources to extract maximum Power.

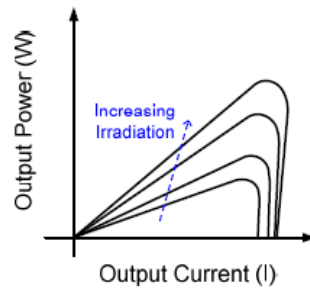


Figure 12: PV Cell Power Characteristics

The HCS strategy perturbs the operating point of the system and observes the output. If the direction of the perturbation (e.g an increase or decrease in the output voltage of a PV array) results in a positive change in the output Power, then the control algorithm will continue in the direction of the previous perturbation.

Conversely, if a negative change in the output Power is observed, then the control algorithm will reverse the direction of the previous perturbation step. In the case that the change in Power is close to zero (within a specified range) then the algorithm will invoke no changes to the system operating point since it corresponds to the maximum Power point (the peak of the Power curves). The MPPT scheme employed in this scheme is a version of the HCS strategy. Figure 13 is the flow chart that illustrates the implemented MPPT scheme.

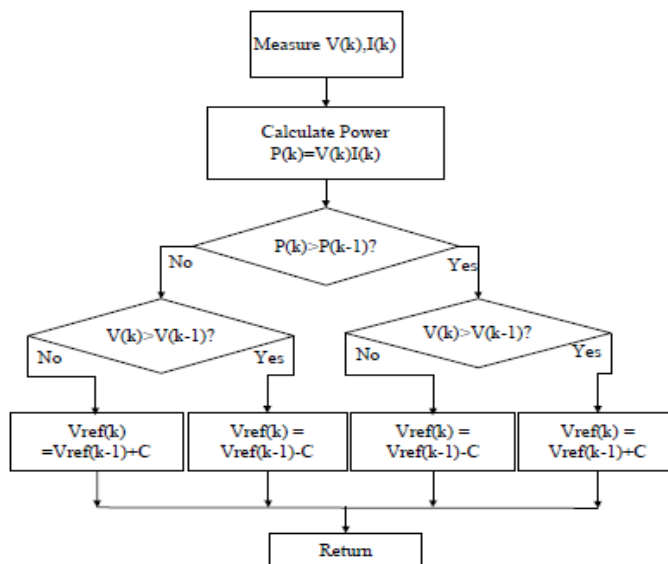


Figure 13: General MPPT Flow Chart for Wind and PV

Results

HYBRID SIMULATION CIRCUIT SYSTEM

The figure 14. represents, Hybrid simulation circuit in this system mainly we are using the SEPIC and CUK converters ,By using this converters additional filters are not necessary. The design specifications are output power is 3KW, output voltage is 500V.

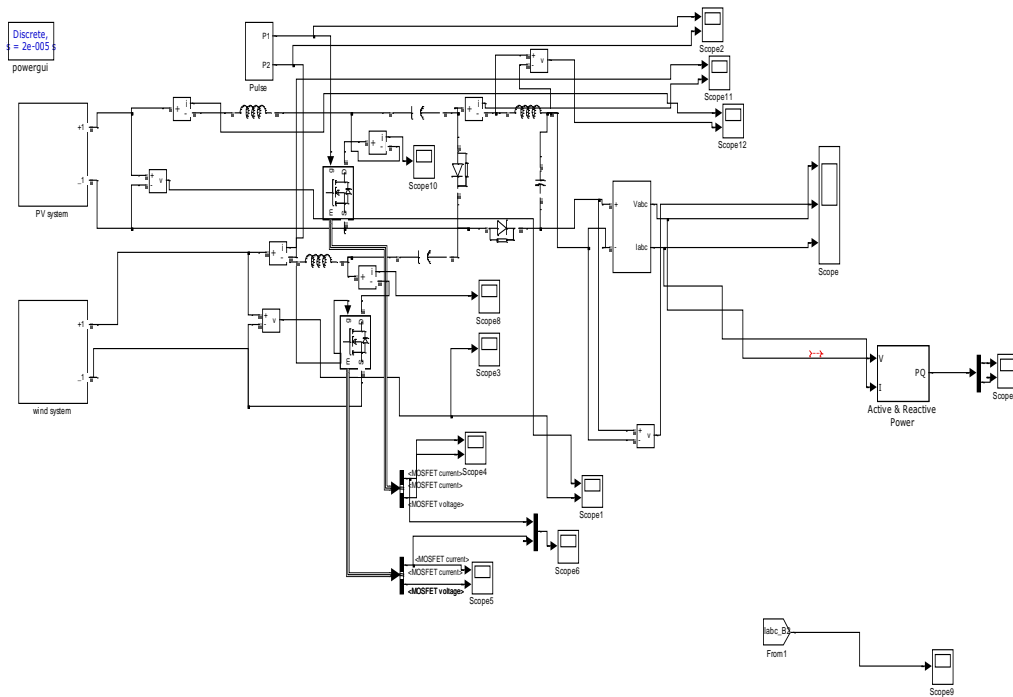


Figure 14 Hybrid System Simulation Circuit

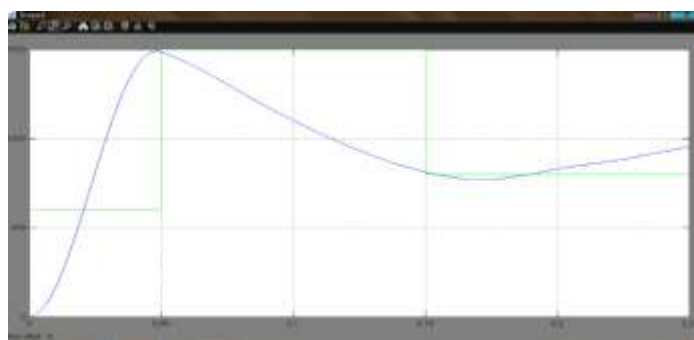


Figure 15.: Solar MPPT – PV output current and reference current signal (Cuk operation)

In the above figure, green colour signal represents reference current signal and blue colour signal represents PV output current signal.



Figure 16: Wind MPPT – Generator speed and reference speed signal (SEPIC operation)

In the above figure, green colour signal represents reference speed signal and blue colour signal represents generator speed signal.

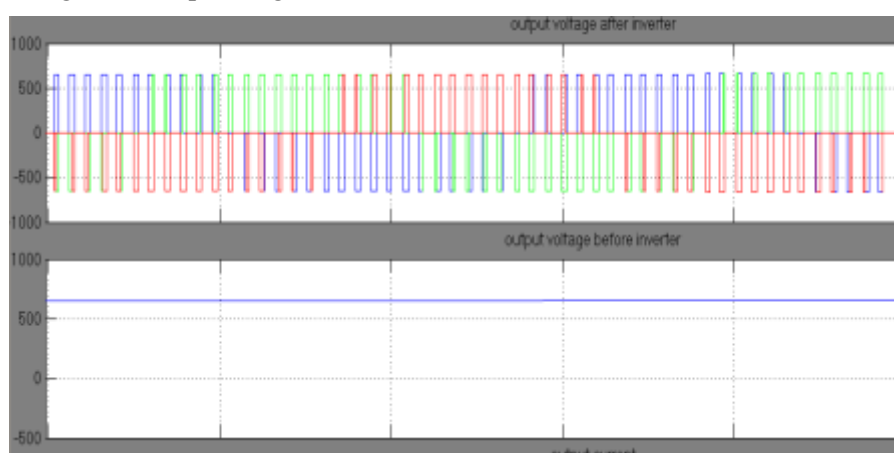


Figure 17: Hybrid inverter Output of Wind & PV

The above figures represents, output voltage after inverter and before inverter, After inverter voltage which is in AC which is almost 500V and before inverter which is in DC, this voltage is constant.

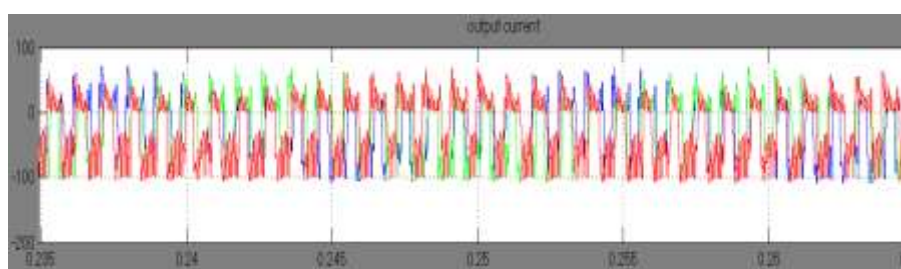


Figure 18: Hybrid output current

The above figures represent, Three Phase Generated Currents and Hybrid output current, Simultaneous operation with both wind and PV source (Fusion mode with Cuk and SEPIC), Hybrid output current is the combination of PV array and wind system

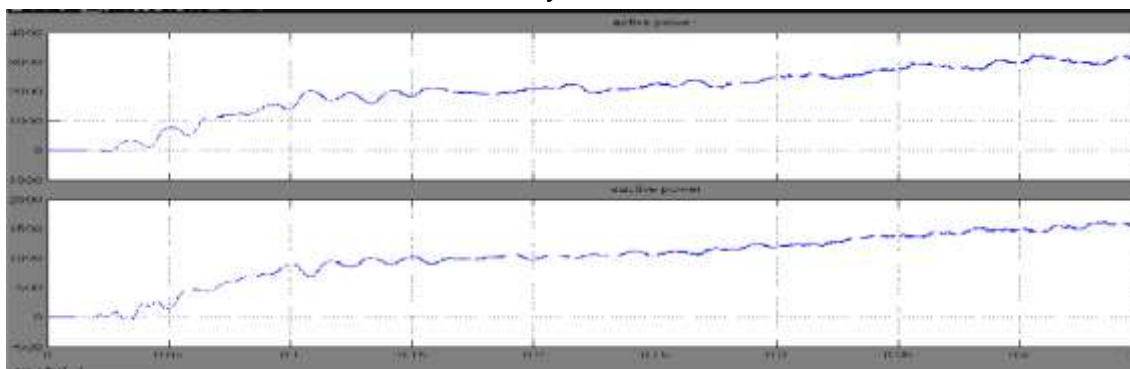


Figure : Active & reactive Power of Hybrid system.

The above figures represent, Active & reactive Power of Hybrid system, Active power with 3KW and reactive power with 1500W.

CONCLUSION

In this project a New Multi Input Cuk-SEPIC Rectifier Stage for Hybrid Wind/Solar Energy systems has been presented. The features of this circuit are, Additional input filters are not necessary to filter out high frequency , reduction in Harmonics. Both renewable sources can be stepped up/down (supports wide ranges of PV and Wind input), MPPT can be realized for each source and Individual and simultaneous operation is supported

REFERENCES

- [1] S.K. Kim, J.H. Jeon, C.H. Cho, J.B. Ahn, and S.H. Kwon, "Dynamic Modeling and Control of a Grid-Connected Hybrid Generation System with Versatile Power Transfer," *IEEE Transactions on Industrial Electronics*, vol. 55, pp. 1677-1688, April 2008.
- [2] D. Das, R. Esmaili, L. Xu, D. Nichols, "An Optimal Design of a Grid Connected Hybrid Wind/Photovoltaic/Fuel Cell System for Distributed Energy Production," in *Proc. IEEE Industrial Electronics Conference*, pp. 2499-2504, Nov. 2005.
- [3] N. A. Ahmed, M. Miyatake, and A. K. Al-Othman, "Power fluctuations suppression of stand-alone hybrid generation combining Solar Photovoltaic/Wind turbine and fuel cell systems," in *Proc. Of Energy Conversion and Management, Vol. 49*, pp. 2711-2719, October 2008.
- [4] S. Jain, and V. Agarwal, "An Integrated Hybrid Power Supply for Distributed Generation Applications Fed by Nonconventional Energy Sources," *IEEE Transactions on Energy Conversion*, vol. 23, June 2008.



- [5] Y.M. Chen, Y.C. Liu, S.C. Hung, and C.S. Cheng, "Multi-Input Inverter for Grid- Connected Hybrid PV/Wind Power System," *IEEE Transactions on Power Electronics*, vol. 22, May 2007.
- [6] dos Reis, F.S., Tan, K. and Islam, S., "Using PFC for harmonic mitigation in Wind turbine energy conversion systems" in *Proc. of the IECON 2004 Conference*, pp. 3100- 3105, Nov. 2004
- [7] R. W. Erickson, "Some Topologies of High Quality Rectifiers" in *the Proc. of the First International Conference on Energy, Power, and Motion Control*, May 1997.
- [8] D. S. L. Simonetti, J. Sebasti'an, and J. Uceda, "The Discontinuous Conduction Mode Sepic and Cuk Power Factor Preregulators: Analysis and Design" *IEEE Trans. On Industrial Electronics*, vol. 44, no. 5, 1997
- [9] N. Mohan, T. Undeland, and W Robbins, "Power Electronics: Converters, Applications, and Design," John Wiley & Sons, Inc., 2003.
- [10] J. Marques, H. Pinheiro, H. Grundling, J. Pinheiro, and H. Hey, "A Survey on Variable-Speed Wind Turbine System," *Proceedings of Brazilian Conference of Electronics of Power*, vol. 1, pp. 732-738, 2003.
- [11] F. Lassier and T. G. Ang, "Photovoltaic Engineering Handbook" 1990.
- [12] Global Wind Energy Council (GWEC), "Global Wind 2008 report," June 2009.
- [13] L. Pang, H. Wang, Y. Li, J. Wang, and Z. Wang, "Analysis of Photovoltaic Charging System Based on MPPT," *Proceedings of Pacific-Asia Workshop on Computational Intelligence and Industrial Application 2008 (PACIIA '08)*, Dec 2008, pp. 498-501.